The Impact of ENSO on Extratropical Low-Frequency Noise in Seasonal Forecasts

SIEGFRIED D. SCHUBERT, MAX J. SUAREZ, AND YEHUI CHANG

NASA Goddard Space Flight Center, Laboratory for Atmospheres, Greenbelt, Maryland

GRANT BRANSTATOR

National Center for Atmospheric Research, Boulder, Colorado

(Manuscript received 14 March 2000, in final form 28 August 2000)

ABSTRACT

This study examines the variability in forecasts of the January–February–March (JFM) mean extratropical circulation and how that variability is modulated by the El Niño–Southern Oscillation. The analysis is based on ensembles of seasonal simulations made with an atmospheric general circulation model (AGCM) forced with sea surface temperatures observed during the 1983 El Niño and 1989 La Niña events. The AGCM produces pronounced interannual differences in the magnitude of the extratropical seasonal mean noise (intraensemble JFM variability). The North Pacific, in particular, shows extensive regions in which the 1989 seasonal mean noise kinetic energy (SKE), which is dominated by a ''Pacific–North American (PNA)–like'' spatial structure, is more than 2 times that of the 1983 forecasts. The larger SKE in 1989 is associated with a larger-than-normal barotropic conversion of kinetic energy from the mean Pacific jet to the seasonal mean noise. The generation of SKE by submonthly transients also shows substantial interannual differences, though these are much smaller than the differences in the mean flow conversions. An analysis of the generation of monthly mean noise kinetic energy and its variability suggests that the seasonal mean noise is predominantly a statistical residue of variability resulting from dynamical processes operating on monthly and shorter timescales.

A stochastically forced barotropic model (linearized about the AGCM's 1983 and 1989 seasonal and ensemble mean states) is used to further assess the role of the basic state, submonthly transients, and tropical forcing in modulating the uncertainties in the seasonal AGCM forecasts. When forced globally with spatially white noise, the linear model generates much larger variance for the 1989 basic state, consistent with the AGCM results. The extratropical variability for the 1989 basic state is dominated by a single eigenmode and is strongly coupled with forcing over the tropical western Pacific and the Indian Ocean. Linear calculations that include forcing from the AGCM variance of the tropical forcing and submonthly transients show a small impact on the variability over the PNA region as compared with that of the basic-state differences.

1. Introduction

It is now well understood that, for the seasonal prediction problem, the mean response of the atmosphere to anomalous boundary forcing is but one aspect of a more general stochastic solution that includes various higher-order moments that define a probability density function (e.g., Barnett 1995; Kumar and Hoerling 1995; Kumar et al. 2000). At the seasonal timescale, the uncertainties due to initial condition errors have equilibrated in the sense that the statistics associated with planetary- and synoptic-scale systems have for the most part lost all memory of the initial conditions. Nevertheless, the equilibrated statistics can be influenced or modulated by slowly varying boundary forcing such as anomalous sea surface temperatures (SSTs). In this study, we examine how tropical SST anomalies associated with ENSO impact the variability of extratropical seasonal forecasts made with an atmospheric general circulation model (AGCM).

The impact of the tropical SST anomalies on the variability of the extratropical response can be direct, for example as a result of changes in variability (uncertainty) of the tropical forcing, or indirect, through changes in the basic state or the variability of subseasonal transients. It is already well established that transients play an important role in the mean extratropical response to ENSO (e.g., Kok and Opsteegh 1985; Held et al. 1989). Several recent studies have focused on how the transients are influenced by and feedback on the ENSO response. For example, Branstator (1995) emphasized the role of selective feedbacks between the transients and forced response. Chen and van den Dool (1997) examined how ENSO impacts subseasonal low-frequency variability over the North Pacific, and show that both blocking and deep trough flows develop twice

Corresponding author address: Dr. Siegfried D. Schubert, Laboratory for Atmospheres, NASA Goddard Space Flight Center, Code 910.3, Greenbelt, MD 20771.
E-mail: schubert@dao.gsfc.nasa.gov

Unauthenticated | Downloaded 03/16/25 08:33 PM UTC

as often over the North Pacific during La Niña as compared with El Niño winters. They further show that the difference in magnitude of the low-frequency variability is the result of increased energy extraction by the low-frequency transients from the mean flow and an enhanced role of high-latitude high-frequency transients in developing and maintaining blocked flows during La Niña winters.

Kumar et al. (2000) employed ensembles of AGCM simulations forced with observed SSTs for the period 1950–94 for four different models to investigate the impact of SST forcing on the second-moment statistics or spread. They find, based on a composite of all warm and cold events, a significant but small reduction in spread over the North Pacific during the warm events and little impact on the spread during cold events. They further suggest that the contribution to seasonal predictability from changes in spread are small compared to the impact of the SST on the mean. Sardeshmukh et al. (2000) analyzed very large ensembles of seasonal mean [January–February–March (JFM)] forecasts generated with the National Centers for Environmental Prediction AGCM for neutral, warm (1987) and cold (1989) ENSO conditions. They found that the geopotential height response is, in general, more variable for the 1987 SST than for the 1989 SST, though both the warm and cold experiments showed increased variability over the North Pacific compared with the neutral ENSO conditions. They speculate that the increased variability in the geopotential height response for 1987 is in part due to increased variability in rainfall in the central equatorial Pacific.

In this study we examine the role of ENSO in modulating the noise (intraensemble variance) of boreal winter forecasts for two cases: the 1983 warm event and the 1989 cold event. We take a case study approach to help to isolate the dominant controls on the variability during extreme events and to avoid averaging different ENSO events that can have quite different atmospheric teleconnection characteristics (e.g., Palmer and Mansfield 1986). We examine the role of the background state, and interannual changes in the intraensemble variance of the tropical forcing and midlatitude transients. The study utilizes ensembles of hindcasts with an early version of the Goddard Earth Observing System (GEOS-2) AGCM. The AGCM results are diagnosed within a kinetic energy framework, and with the aid of a stochastically forced barotopic model linearized about the AGCM ensemble mean states.

Section 2 gives an overview of the AGCM and forecast experiments. The AGCM results are presented in section 3. The results of the stochastically forced barotropic model linearized about the AGCM ensemble mean flow are presented in section 4. The summary and conclusions are given in section 5.

2. The model and forecast experiments

The AGCM is an early version of the GEOS-2 model described in (Chang et al. 2000). It has 43 sigma levels extending up to 10 mb and a horizontal resolution of 2° latitude by 2.5° longitude. The seasonal mean ENSO response of this model is described in Chang et al. (2000) based on an ensemble of nine forecasts starting in mid-December for each winter season (JFM) for the period 1981–95. The results of that study suggest that the JFM mean ENSO response in the GEOS-2 model tends to be weak. In fact, a comparison of the JFM mean ENSO response in a number of different models (Shukla et al. 2000) shows a wide range of signal-to-noise ratios over the Pacific–North American (PNA) region. Here, the signal-to-noise ratio is defined as the ratio of the interensemble variance (the variance of the ensemble means) to the intraensemble variance. The issue of model dependence and its potential impact on the results of this study is addressed in the conclusions.

Ensembles of 5–10 members, typical of many previous AGCM experiments focusing on the ensemble mean response, may be too small to obtain reliable higher-moment statistics. In this study, we generate ensembles with 27 members to provide more reliable estimates of the second-moment statistics. The issue of statistical significance will be discussed in the next section. The initial conditions are based on the GEOS-1 reanalysis (Schubert et al. 1993). The 27 perturbations to the initial conditions are generated by taking the difference between two randomly chosen December states separated by 12 h, and adding that difference to the 15 December (1982 or 1988) base state (see Schubert and Suarez 1989).

In all AGCM experiments described here, the SST and sea ice are prescribed using observed monthly boundary conditions (Reynolds and Marsico 1993). Soil moisture is prescribed as described in Chang et al. (2000).

3. AGCM results

As described in Quiroz (1983), the warm event of 1982/83 was one of the strongest El Niño episodes of the century with the lowest recorded value of the Southern Oscillation index (3.5 standard deviations below normal) since 1935, and DJF sea surface temperature anomalies exceeding 3°C over much of the eastern equatorial Pacific. The wintertime Northern extratropics were characterized by an unusually deep Aleutian low, an enhanced and eastward-extended Pacific jet, and a positive height anomaly over the Atlantic–Eurasian sector. Cyclone tracks and the jet over the Pacific and United States were south of their normal position, while major wintertime blocking episodes were confined to the Atlantic and European sectors.

The cold event during DJF 1988/89 was characterized by SSTs of more than 1° below normal throughout the central and eastern equatorial Pacific (e.g., Arkin 1989). Large positive height anomalies (exceeding 120 m) occurred over the eastern North Pacific acting to divert weather systems to the north of their usual tracks. The

Unauthenticated | Downloaded 03/16/25 08:33 PM UTC

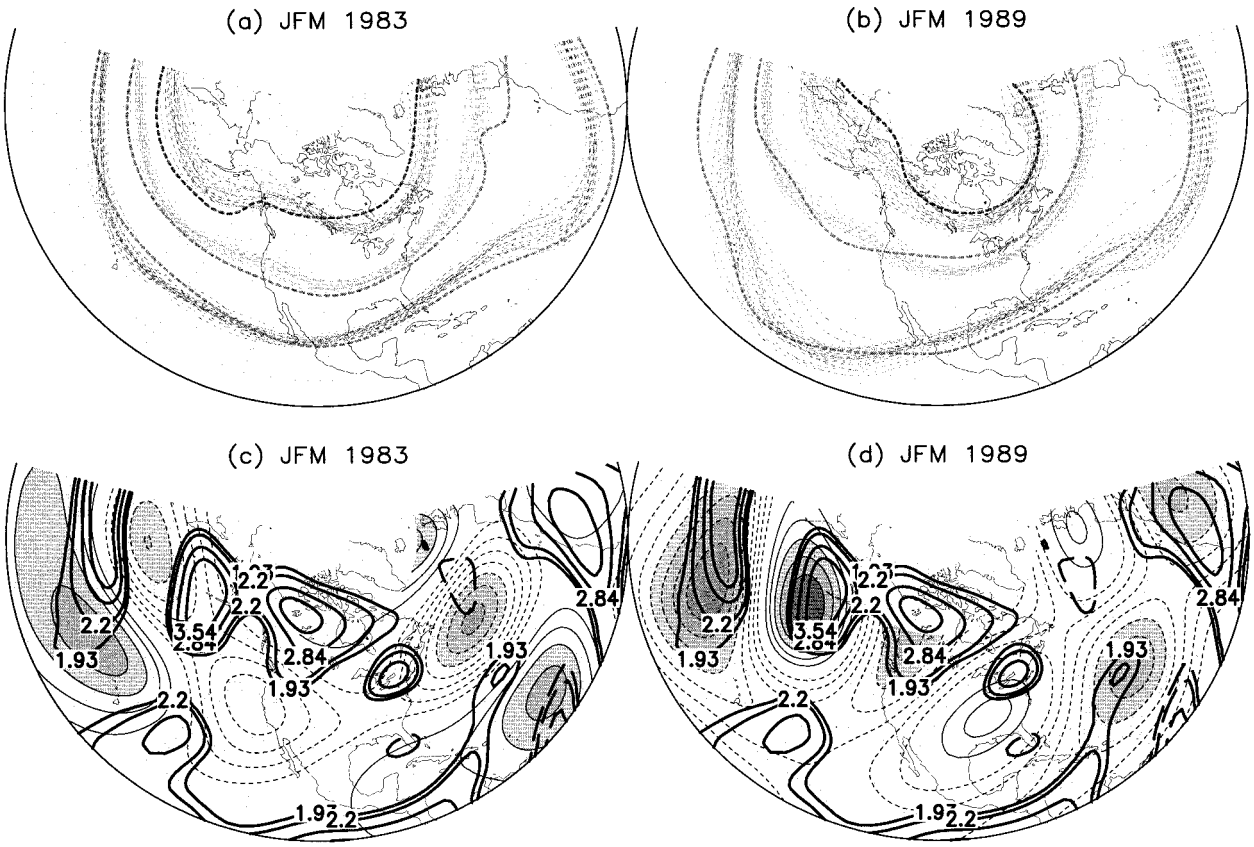

FIG. 1. Three arbitrarily chosen JFM mean streamlines at 200 mb for all 27 ensemble members of the AGCM hindcasts (thin dashed lines) and the observations (thick dashed lines) for (a) 1983 and (b) 1989. The dominant EOF of the 200-mb streamfunction of the AGCM JFM mean noise (computed for the region shown) for (c) 1983 and (d) 1989. The heavy lines in (c) and (d) show the ratio of the 1989 JFM noise variance to the 1983 JFM variance. Contour levels show the 10%, 5%, 1%, and 0.2% two-sided significant levels (solid lines indicate regions where 1989 variance is larger than 1983 variance, and dashed lines indicate the reverse).

east Pacific anomaly was part of a larger-scale anomaly pattern consisting of above-normal heights at 500 mb in the midlatitudes and below-normal heights over the poles in both the Northern and Southern Hemispheres. Considerable month-to-month variability occurred over the United States with near-normal temperatures in December, very warm in January, and very cold in February.

a. Description of variability

The mean circulation anomalies for JFM of 1983 and 1989 are depicted in Figs. 1a and 1b in terms of selected isolines of streamfunction or streamlines of the 200-mb nondivergent wind. The heavy lines are the observed values from the GEOS-1 reanalysis. The thin lines are from the 27 model hindcasts. Both the observations and model JFM hindcasts show the large differences during these two events over the eastern North Pacific discussed above and reflected here in the largely zonal flow extending across the Pacific into the western United States during the warm event and the strongly diffluent flow during the cold event.

Another major difference between the two events is in the AGCM's intraensemble spread in the streamlines. The 1983 warm event shows a close packing of the JFM streamlines over the central and eastern North Pacific, while for the 1989 cold event there is considerable intraensemble spread. This indicates a substantially greater variability in the hindcasts of the cold event in the diffluent regions of the North Pacific. Over the North Atlantic, there is some tendency for the flow to be more diffluent and the variability to be larger during 1983. The observed JFM streamlines lie near the edge of the model's range of outcomes reflecting the model's tendency to produce a weaker-than-observed response to the SST anomalies (Chang et al. 2000).

The spread of the ensemble members shown in Figs. 1a and 1b can be quantified in terms of the intraensemble variance of the JFM mean fields. We refer to this as the seasonal mean noise. Figures 1c and 1d shows the dominant EOFs of the seasonal mean noise in the 200-mb streamfunction for 1983 and 1989, respectively. The dominant EOF in 1983 has a strong component in the North Atlantic sector reflecting the somewhat larger variance in that region as compared with the Pacific during

Unauthenticated | Downloaded 03/16/25 08:33 PM UTC

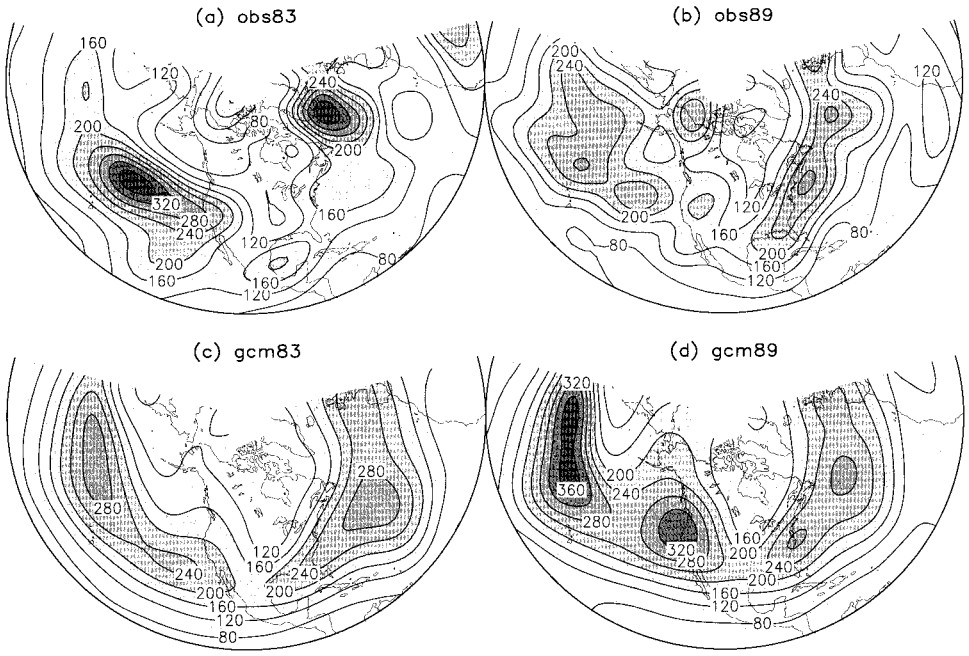

FIG. 2. Submonthly variance of the 200-mb streamfunction for JFM computed from the GEOS-1 reanalyses for (a) 1983 and (b) 1989. The AGCM submonthly JFM variance of the 200-mb streamfunction averaged over the 27 hindcasts for (c) 1983 and (d) 1989. Units: $(m^2\ s^{-1} \times 10^6)^2$.

this year. This mode explains 30% of the intraensemble variance. The north–south dipole at high latitudes and the zonally elongated structure of the EOF are features that bear some resemblance to the western North Atlantic pattern found in the observations on monthly and longer timescales (Wallace and Gutzler 1981). In the Pacific the EOF also shows a north–south structure and zonally elongated anomalies. We note that the second EOF shows a structure that resembles the PNA pattern (Wallace and Gutzler 1981). During 1989, the dominant EOF of the intraensemble variance of the JFM mean streamfunction shows a well-defined PNA structure. This mode explains 38% of the intraensemble variance.

The test for determining the statistical significance of the differences in the intraensemble variability between the two years is based on the *F* distribution (e.g., DeGroot 1975). With 27 ensemble members, and under the null hypothesis that the variances for 1983 and 1989 are the same, the ratio of the unbiased variance estimates has an *F*(26, 26) distribution. The ratio of the 1989–83 total intraensemble variance (Figs. 1c and 1d) shows clearly that the significant extratropical differences in variability between the two years are largely due to the greater variability of the PNA mode during 1989. We note that the region of enhanced variability over the North Atlantic during 1983 is only marginally significant.

We next take a brief look at the variance of the subseasonal transients, how it compares with the observed variance, and its intraensemble variability. As we shall see, it is the latter that potentially impacts the interannual differences in the seasonal noise. Figure 2 compares the observed and AGCM submonthly variability of the 200 mb streamfunction. The submonthly variance is computed from the deviations about the monthly means using 6-hourly output. Variability on timescales longer than one month but shorter than one season does not contribute significantly to the kinetic energy conversion terms (see below), so we do not include it here. The AGCM results are the average variances from all 27 ensemble members, while the observations are of course from a single realization. Both the model and observations show substantial differences in the submonthly variability over the eastern North Pacific and western North America. During 1983, the highest variability occurs in a narrow latitudinal band extending across the Pacific into North America, while during 1989 the region of high variability has a greater latitudinal range, extending well north of 60°N. Both the model and observations show a tendency for greater variability in the North Atlantic in 1983, though in the observations the region of maximum variability lies farther to the north. In the model, the largest variability occurs in 1989 in the Pacific storm track between Japan and Hawaii, and over the western United States. We note that both the model and observations show higher submonthly variability during 1989 extending southward into the Tropics throughout the eastern Pacific (not shown), suggesting greater propagation into the Tropics during this year.

Unauthenticated | Downloaded 03/16/25 08:33 PM UTC

It is difficult to determine whether the differences in submonthly variability between the model and observations reflects sampling variability or model errors. Many of the localized features may be due to sampling differences. That is, the noiser structure in the observations likely reflects the occurrence of just a few events during JFM, while the model results include transients from 27 different JFM realizations. For example, the large but localized region of submonthly variability observed over the North Atlantic during 1983 is not evident in the average statistics from the AGCM. To help sort out these differences we have computed the intraensemble standard deviation of the AGCM submonthly variance (not shown). We find that large intraensemble variability of the submonthly variability occurs over much of the North Pacific and west coast of the United States during 1989, suggesting that the differences with the observations in this region may be due to sampling variability. The intraensemble variability of the submonthly variability tends to be smaller during 1983; however, the region of large discrepancy between model and observations in the North Atlantic does tend to be a region of enhanced intraensemble variability.

b. Energy conversions

In the following, we examine the nature of the interannual differences in the JFM noise variance using a kinetic energy framework. The ensemble mean seasonal mean noise kinetic energy (SKE) or intraensemble variability is defined as

$$\text{SKE} = 1/2\langle \overline{u}^{*2} + \overline{v}^{*2} \rangle, \tag{1}$$

where the star denotes a deviation from the ensemble mean, the angle bracket denotes an ensemble mean, the overbar is a seasonal (JFM) mean, and u and v are the spatially varying zonal and meridional wind components. Figure 3 compares the SKE at 200 mb for 1983 and 1989. Consistent with Fig. 1, pronounced interannual differences in SKE occur over the North Pacific, with 2 to 3 times more SKE during 1989 over considerable portions of the PNA region (Fig. 3c). On the other hand, over the North Atlantic there was more SKE during 1983, although the differences between the two years are smaller, and the overall magnitudes are considerably less than the 1989 North Pacific values. Values of the ratio of 1989 to 1983 SKE that are greater (less) than 1.6 (0.64) are locally significant at the 5% level (see the appendix). However, only the values greater than 1.6 occur over a sufficiently large area to have field significance at the 5% level.

The local barotropic conversion terms (e.g., Simmons et al. 1983) in the equation governing the SKE are approximately

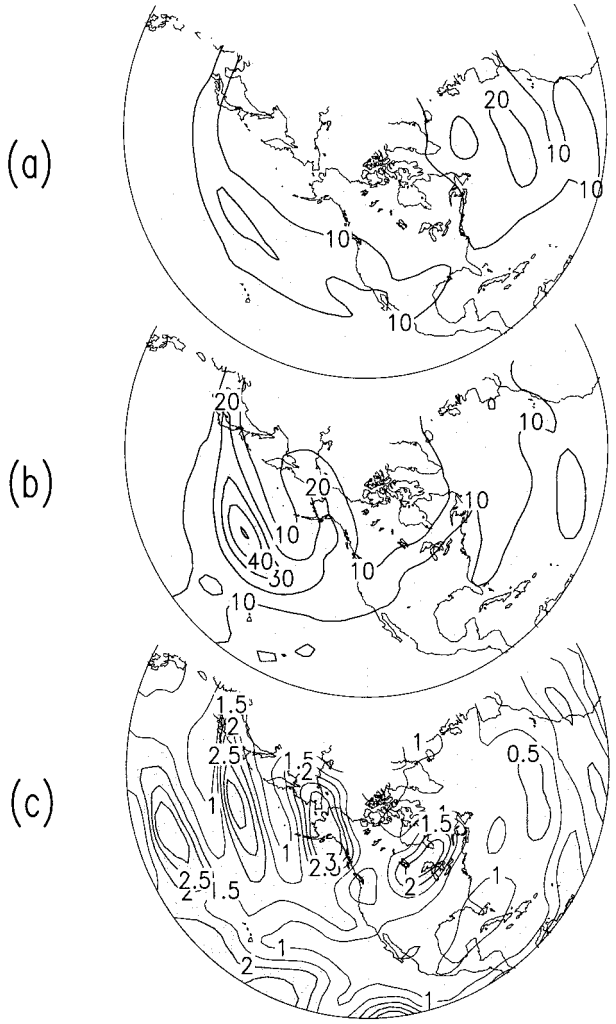

FIG. 3. JFM ensemble mean SKE at 200 mb computed from the 27 AGCM hindcasts for (a) 1983 and (b) 1989. Units: $m^2\ s^{-2}$. (c) The ratio of the 1989-to-1983 200-mb SKE. Values greater than 1.6 and less than 0.64 are shaded.

$$\text{C1} = -\langle \overline{u}^{*2} - \overline{v}^{*2} \rangle \frac{\partial \langle \overline{u} \rangle}{\partial x} - \langle \overline{u}^{*} \overline{v}^{*} \rangle \frac{\partial \langle \overline{u} \rangle}{\partial y} - \langle \overline{u}^{*} \overline{v}^{*} \rangle \frac{\partial \langle \overline{v} \rangle}{\partial x} \simeq \mathbf{E} \cdot \nabla \langle \overline{u} \rangle, \quad \text{and} \tag{2a}$$

$$\text{C2} = \left\langle (\overline{u'^2} - \overline{v'^2})^{*} \frac{\partial \overline{u}^{*}}{\partial x} \right\rangle + \left\langle \overline{u'v'}^{*} \frac{\partial \overline{u}^{*}}{\partial y} \right\rangle + \left\langle \overline{u'v'}^{*} \frac{\partial \overline{v}^{*}}{\partial x} \right\rangle. \tag{2b}$$

Here, the prime denotes a deviation from the seasonal mean, and the star and overbar are as in (1) above. Term C1 is the conversion of kinetic energy from the ensemble mean flow to the SKE, and C2 is the conversion of kinetic energy from the subseasonal transients to the SKE. We will also refer to C1 as the generation of SKE

Unauthenticated | Downloaded 03/16/25 08:33 PM UTC

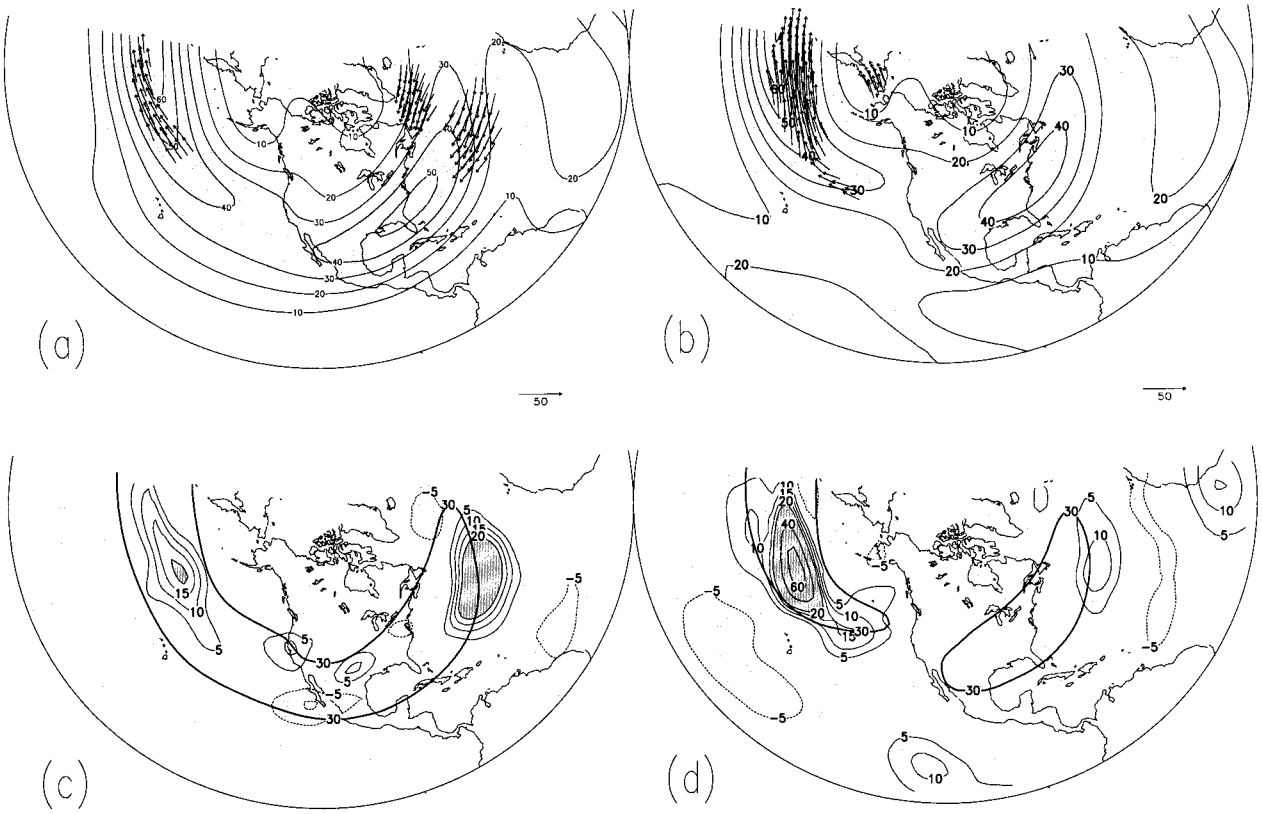

FIG. 4. The AGCM ensemble mean JFM 200-mb zonal wind with superimposed **E** vectors ($m^2\ s^{-2}$) of the seasonal mean noise at 200 mb for (a) 1983 and (b) 1989, and the mean flow generation term (C1 in text) for (c) 1983 and (d) 1989. The contour levels in (a) and (b) are 10 m s^{-1}. Values greater than 30 m s^{-1} are shaded. In (c) and (d) the heavy contour is a repeat of the 30 m s^{-1} contour of the zonal wind field for each year. Contour intervals are ± 5, 10, 15, 20, 40, 60. Negative values have dashed contours. The light shading indicates values of C1 less than $-5\ m^2\ s^{-2}\ day^{-1}$ and the dark shading indicates values larger than $20\ m^2\ s^{-2}\ day^{-1}$.

due to the mean flow, and C2 as the generation of SKE due to the subseasonal transients. The approximate form of C1 in (2a) is obtained by dropping the term involving the zonal gradient in the mean meridional wind, which tends to be small (Simmons et al. 1983). The **E** vector (Hoskins et al. 1983) is defined here for the seasonal mean intra-ensemble anomalies as

$$\mathbf{E} = -\langle \overline{u}^{*2} - \overline{v}^{*2} \rangle \mathbf{i} - \langle \overline{u}^{*}\overline{v}^{*} \rangle \mathbf{j}. \qquad (3)$$

From the simplified form of C1 it is clear that when the **E** vectors point in the direction of the gradient of the mean zonal wind there is a growth of SKE. In the case of C2, the generation of SKE occurs if the **E** vectors of the subseasonal transients (not shown) tend to point in a direction opposite to the gradient of the seasonal mean zonal wind anomalies.

Figures 4a and 4b show the **E** vectors of the seasonal mean noise [(3)] superimposed on the ensemble mean 200-mb zonal winds for 1983 and 1989, respectively. During 1983 the Pacific jet (winds greater than 30 m s^{-1}) extends eastward across North America to connect with the Atlantic jet. In contrast, during 1989 the Pacific jet is retracted westward with enhanced winds just off the east Asian coast resulting in strong zonal gradients in the zonal wind in the central Pacific. Also, in 1989 the Atlantic jet is weaker and shifted to the north compared to 1983. In both years, the **E** vectors are directed toward increasing zonal wind in the Pacific jet exit region, indicating a generation of SKE due to the mean flow. Larger **E** vectors during 1989, together with the stronger zonal wind gradients associated with the retracted Pacific jet, result in a much larger generation of SKE during 1989 (Fig. 4d). In the Atlantic sector, the larger generation of SKE occurs during 1983 in association with the stronger Atlantic jet during that year (Fig. 4c).

The generation of SKE due to the subseasonal transients (term C2) is shown in Fig. 5. We consider only the submonthly transients (Figs. 5a and 5b), because the contribution from transients with timescales between one month and one season (not shown) is small: absolute values are less than 6 $m^2\ s^{-2}\ day^{-1}$ almost everywhere and approach 15 $m^2\ s^{-2}\ day^{-1}$ in only a very small region over the North Pacific in 1989. Here C2 tends to be positive and largest in the jet exit regions and over the eastern oceans. As compared with C1, these conversion terms tend to be small. It is noteworthy, however, that the maxima in C2 tend to occur farther to the

Unauthenticated | Downloaded 03/16/25 08:33 PM UTC

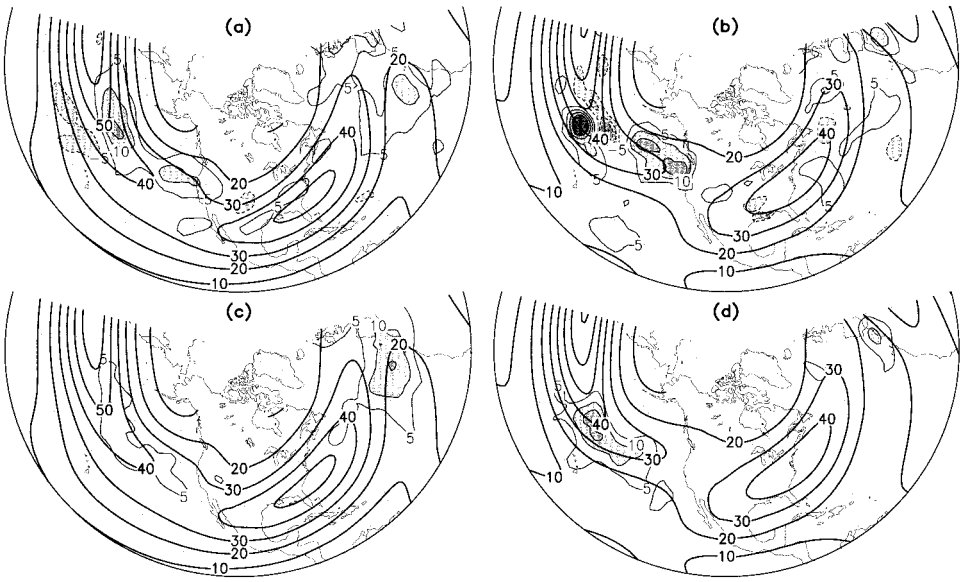

FIG. 5. The generation of SKE for 1983 by (a) the submonthly transients (C2 in text) and (c) the short-period transients (periods < 10 days). (b), (d) The same, but for 1989. Contour intervals are ± 5, 10, 15, 20, 40 $m^2\ s^{-2}\ day^{-1}$. Negative values have dashed contours.

east. Figures 5c and 5d show the contribution to C2 by weather systems alone (timescales less than 10 days). The strong resemblance to the contribution from the full submonthly variations, suggests that much of the conversion is accomplished by the short-period (weather) transients. The main exception is in the Gulf of Alaska where variability with timescales longer than 10 days provides the greatest contribution to the kinetic energy conversion.

c. Analysis of timescales

While the above results suggest that barotropic conversion from the mean flow is an important source of SKE, it is possible that the noise is actually generated on shorter timescales (e.g., monthly), and that the seasonal mean intraensemble variability is primarily a sampling artifact of subseasonal intraensemble variability. To address this question, we compare the kinetic energy of the seasonal mean noise (SKE) with the kinetic energy of the monthly mean noise (MKE). If each seasonal mean were simply an average of three uncorrelated monthly means, the SKE would be equal to the MKE/3. Figures 6a and 6b show that this is approximately true (cf. Figs. 3a and 3b). During both years the values of the ratio SKE/(MKE/3) lie almost everywhere between 0.8 and 1.4. In particular, less than 10% of the area has ratios larger than 1.4. While values larger than 1.27 (the local 5% significance value) have field significance at the 5% level (see the appendix), we nevertheless conclude that much of the variance of the seasonal means is a statistical residual or sampling artifact of variance on monthly and shorter timescales.

The implication of the above results is that, for much of the variability, the underlying dynamical processes are acting, not on seasonal timescales but, on monthly and shorter timescales. The timescales associated with the barotropic generation from the mean flow in linear calculations is rather sensitive to the basic state (e.g., Simmons et al. 1983; Borges and Sardeshmuhk, 1995; section 4). Observations show that the barotropic generation from the mean flow tends to be positive for anomalies with timescales as short as 20 days, though the efficiency of the conversion is greater for lower-frequency modes (Schubert 1986). In fact, Palmer (1988) suggests that barotropic instability of the atmosphere is important for determining the skill of medium- and extended-range weather forecasts. Also, nonmodal growth of decaying normal modes can lead to large energy increases over short time intervals (Borges and Sardeshmuhk 1995; Sardeshmukh et al. 1997). While it is beyond the scope of this paper to determine the dominant timescales of low-frequency variability (see also Feldstein 2000), our point here is that understanding the nature of the seasonal noise requires understanding dynamical processes that generate variability on timescales substantially shorter than one season. Figure 7 shows, for example, the generation of MKE due to energy conversion from the submonthly transients and the mean flow. The results are, to a large extent, similar to those found for SKE. The generation of MKE from the mean flow over the North Pacific is much larger during 1989 than during 1983. The reverse is true over the North Atlantic. Also, the contribution from the submontly transients over the North Atlantic is larger during 1983 compared with 1989, however, this term is again substantially smaller than the conversion from the mean flow.

Unauthenticated | Downloaded 03/16/25 08:33 PM UTC

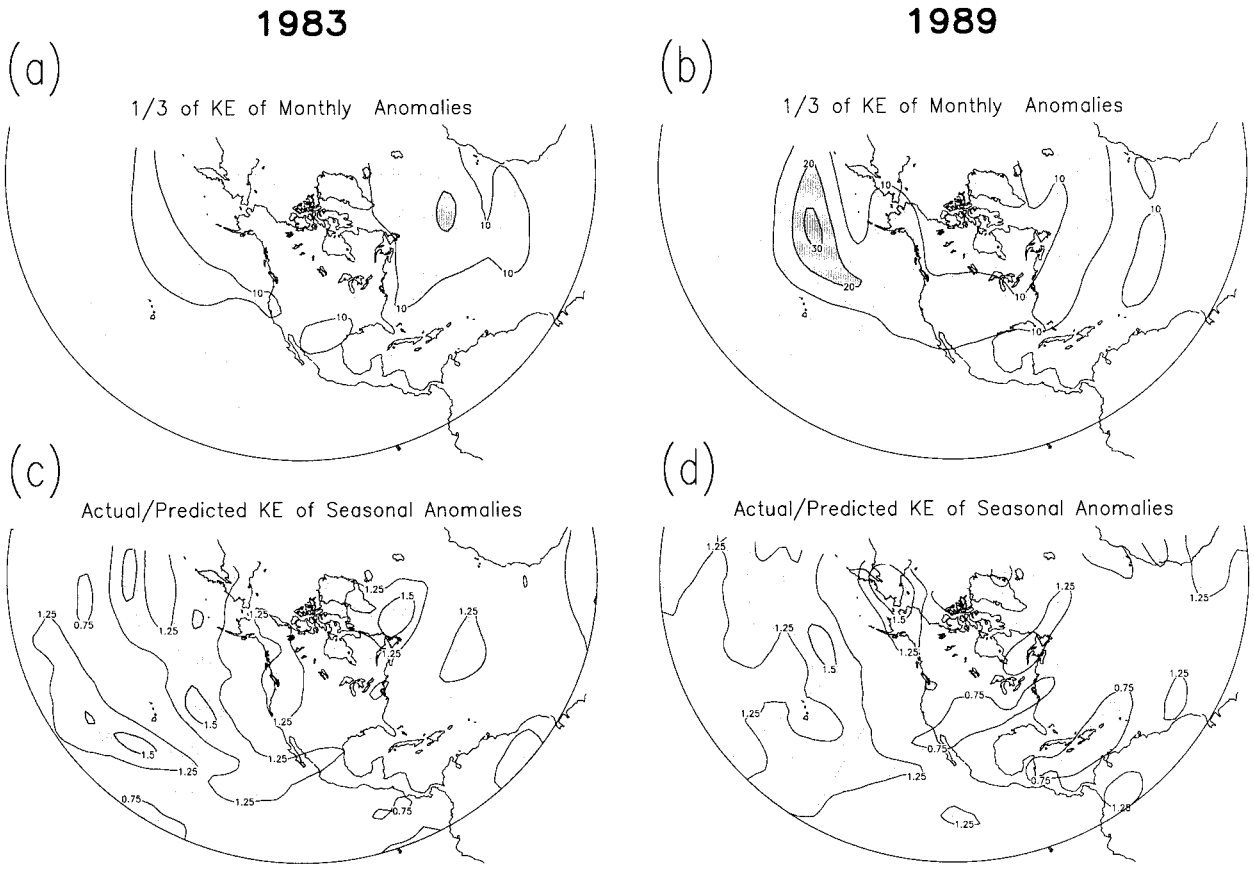

FIG. 6. One-third of the ensemble mean monthly mean noise kinetic energy at 200 mb for (a) 1983 and (b) 1989. Units: $m^2\ s^{-2}$. Values greater than 10 are shaded. The ratio of the actual to the predicted (one-third the monthly) ensemble mean seasonal mean noise kinetic energy for (c) 1983 and (d) 1989. The contour interval is 0.25. Values less than 0.75 and greater than 1.27 are shaded.

4. Linear model results

The linear model (Branstator 1985) is the nondivergent barotropic vorticity equation linearized here about a basic state obtained from the GEOS-2 AGCM hindcasts. The model is discretized using spherical harmonics truncated at R15 and steady solutions are directly solved for using matrix operations. The model has second-order diffusion with a coefficient of $2.5 \times 10^{-5}\ m^2\ s^{-1}$. There is also Rayleigh damping with a coefficient of 3.86×10^{-6}, which corresponds to a damping time of 3 days. The damping, while somewhat stronger than typically used, is not inconsistent with data (Klinker and Sardeshmukh 1992).

For the cases presented here, to be consistent with the analysis of the previous section we linearize about the 200-mb streamfunction, though the calculations have also been done at 300 mb, and all of the conclusions we reach are unchanged. For convenience, we shall, in the following, refer to the streamfunction field about which the model is linearized as the basic state. Linear calculations are carried out using three states: the 1983 and 1989 AGCM seasonal and ensemble means, and a control state consisting of the average of the 15-yr (1981–95) by 9-member ensembles generated previously with the GEOS-2 model (Chang et al. 2000).

For later comparison with the linear calculations, Fig. 8 shows the global distribution of the 200-mb streamfunction standard deviation (superimposed on the zonal wind) obtained from the AGCM. This shows that, in addition to the variability over the North Atlantic and Pacific Oceans already discussed, considerably variability (also enhanced in 1989) occurs in the jet entrance region of the Pacific jet centered near 70°E.

a. Impact of the basic state

To assess the impact of the basic state, we obtain ensembles of linear solutions using stochastic forcing. We first consider forcings that are white and homogeneous in space. For any particular solution, the forcing at each grid point is found by drawing from a uniform random distribution with values ranging from -1 to 1. For each basic state, the linear calculations are repeated 500 times, obtaining the stationary response to 500 different forcing fields. At each grid point, we compute the variance over this ensemble of 500 solutions to com-

Unauthenticated | Downloaded 03/16/25 08:33 PM UTC

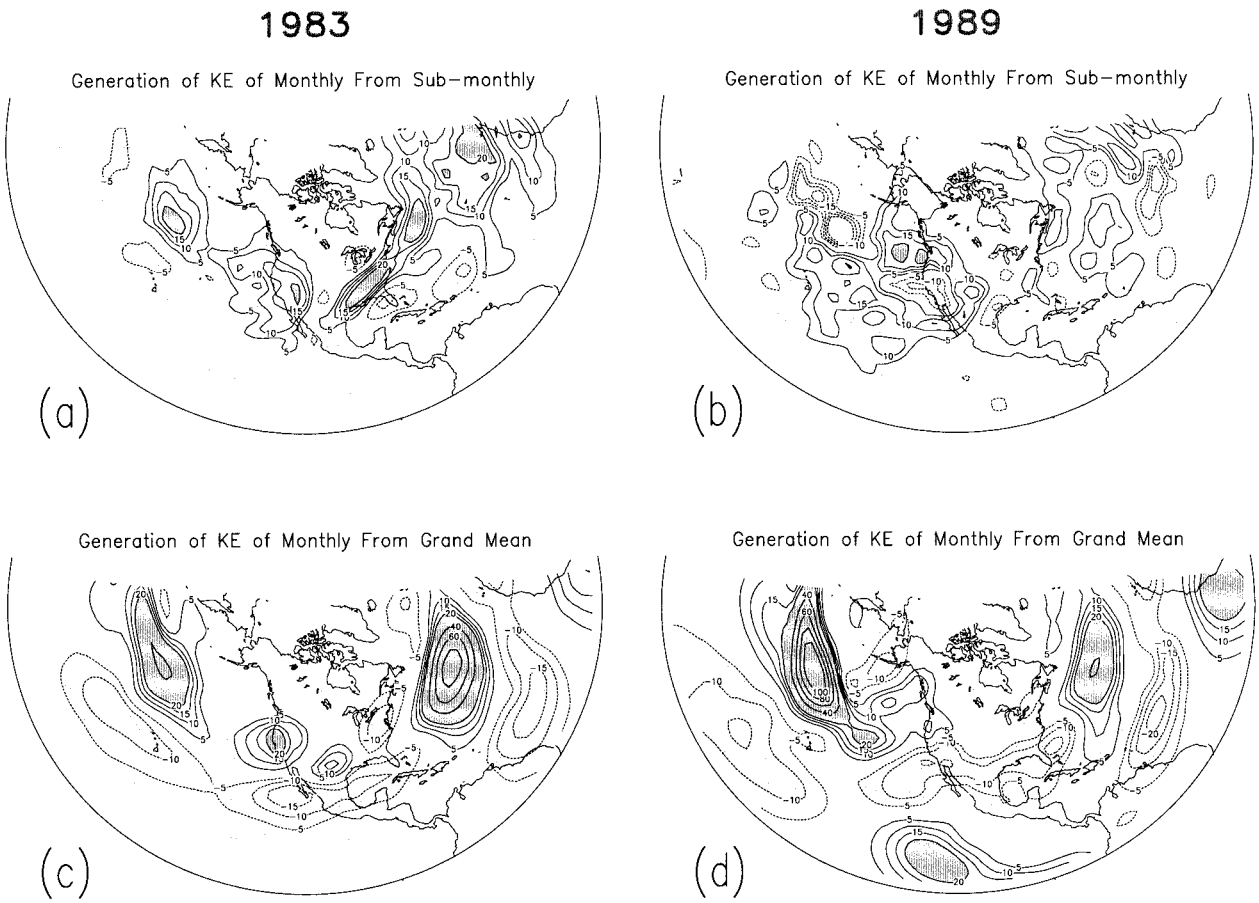

FIG. 7. Generation of monthly mean noise kinetic energy for 1983 by (a) submonthly transients and (c) the mean flow. (b), (d) The same, but for 1989. Contour intervals are ± 5, 10, 15, 20, 40, 60, 80, 100 $m^2\ s^{-2}\ day^{-1}$. The light shading indicates values less than -5 and the dark shading indicates values larger than 20.

pare with the intraensemble variance (noise) of our nonlinear AGCM results. As described in Dymniikov and Filatov (1989) and Branstator (1990), the set of solutions with completely unorganized forcing provides information about the role of barotropic dynamics and the climatological mean state in giving structure to low-frequency perturbations. We note that for all the linear model solutions presented in this section, no attempt was made to scale the forcing to make it physically reasonable; therefore, the unit of the standard deviation is arbitrary.

Figure 9 shows the standard deviation of the streamfunction from the 500 linear calculations with the homogeneous white noise forcing for the 1983, 1989, and the control basic states. The control (Fig. 9c) shows broad maxima in variance over the North Pacific, North Atlantic, and south Asia. These are broadly similar to the regions of high variance found in the AGCM (cf. Fig. 8c). The 1983 variance is similar to that of the control in both magnitude and distribution, although there is somewhat less variance over the North Pacific. Consistent with the AGCM results, 1989 (Fig. 9b) shows considerably more variance than either 1983 or the control, though the locations of the maxima differ from those of the AGCM. For example, the large maxima over the North Pacific are further east in the linear model solutions, and the high-latitude Aleutian maximum is absent from the linear calculations.

The localized nature of the regions of large variance for 1989 suggests the variability for this year might be dominated by a single mode. This is confirmed in Fig. 10a that shows the dominant eigenmode of the linear operator using the 1989 ensemble mean as a basic state. This mode has an *e*-folding time of 6.6 days (in the absence of damping) and it is stationary. For comparison, the fastest growing mode for the control basic state is stationary and has an *e*-folding time of 16.3 days. For the 1983 basic state, it *e*-folds in 17.6 days and has a period of 2130 days. For the control and 1983 basic states, no single mode dominates the variance.

A singular value decomposition (SVD; Bretherton et al. 1992) between the random forcing and the linear solutions for 1989 (SVD 1 in Figs. 10b and 10c) shows that forcings over Indonesia and Indian Ocean are most responsible for the midlatitude response. SVD 1 explains 19.4% of the covariability. This contrasts with

Unauthenticated | Downloaded 03/16/25 08:33 PM UTC

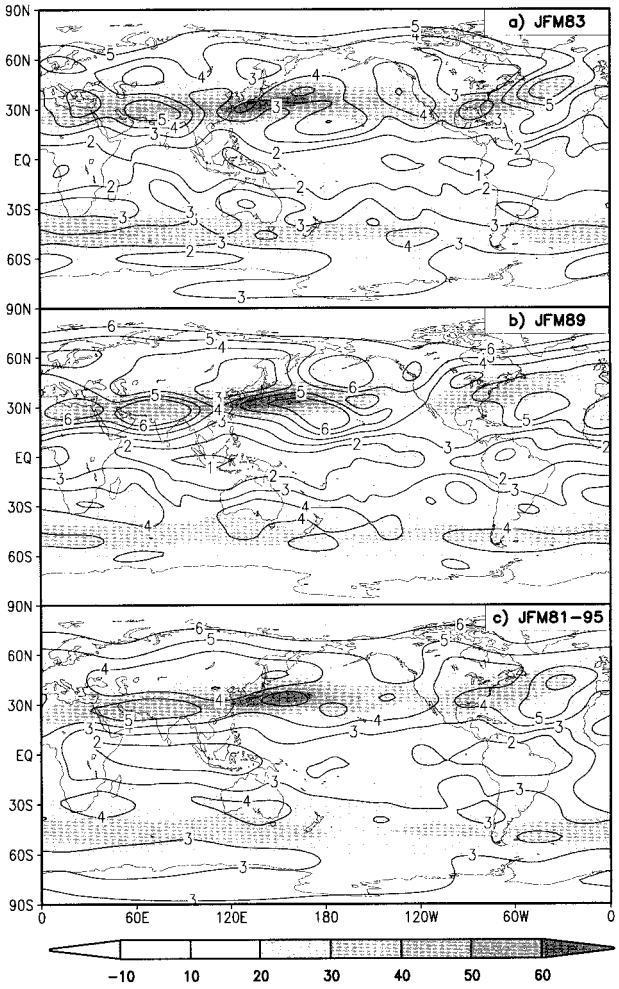

FIG. 8. Global distribution of the AGCM JFM ensemble mean 200-mb zonal wind (shaded), and the JFM streamfunction intraensemble standard deviation or noise (contoured) for (a) 1983, (b) 1989, and (c) 1981–95. The wind has units of meters per second and the contour interval for the noise is 10^6 m^2 s^{-1}. The values in (c) are based on 9-member ensembles for each year. The 1983 and 1989 values are based on 27 ensemble members.

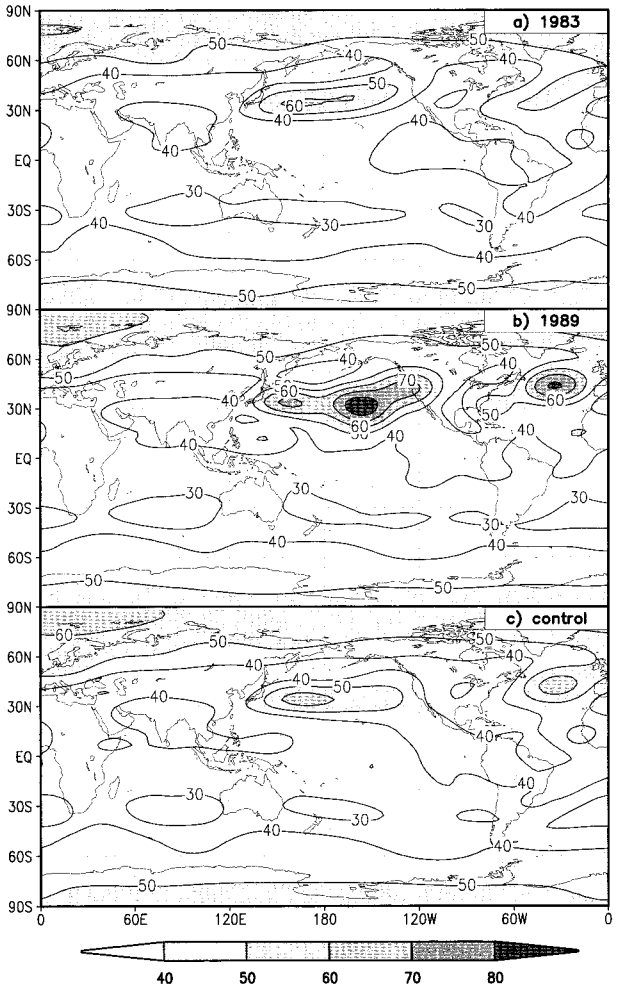

FIG. 9. Standard deviation of the streamfunction from the linear model solutions with global white noise forcing for (a) the 1983 basic state, (b) the 1989 basic state, and (c) the control (1981–95) basic state. Contour intervals are the same in each panel but arbitrary.

the control and 1983, for which the first SVDs (not shown) explain only 8.6% and 8.4% of the covariability, respectively.

b. Impact of tropical precipitation variability

The results of the previous section show that the interannual differences in the midlatitude variance of seasonal means may be, at least in part, attributed to interannual differences in the basic state. It is also possible, however, that interannual differences in the forcing—rather than the basic state—may be contributing to the differences. To test this hypothesis, we repeat the experiments of the previous section, but with a modified stochastic forcing.

Clearly, there are large differences in the *mean* tropical forcing between 1983—an El Niño year—and 1989—a La Niña year. In the GCM results, these are reflected in the difference ensemble mean extratropical responses found for the two years. In addition, however, the *intraensemble variance* or ''noise'' of the forcing is also different in the two years. This is illustrated by the intraensemble variances of the JFM mean precipitation shown in Fig. 11. These changes in the intraensemble variance largely follow changes in the mean itself. Note, for example, the greater variance of precipitation in the eastern tropical South Pacific for the warm event (1983), while for 1989 a larger variance occurs over the Indian Ocean. To mimic these differences in the AGCM forcing in linear calculations, we construct families of forcing functions that take into account the three precipitation noise distributions shown in Fig. 11. Using the assumption that tropical precipitation anomalies produce upper-tropospheric divergence anomalies of identical horizontal structure and taking into account only the vorticity stretching that would result, we form forcing

Unauthenticated | Downloaded 03/16/25 08:33 PM UTC

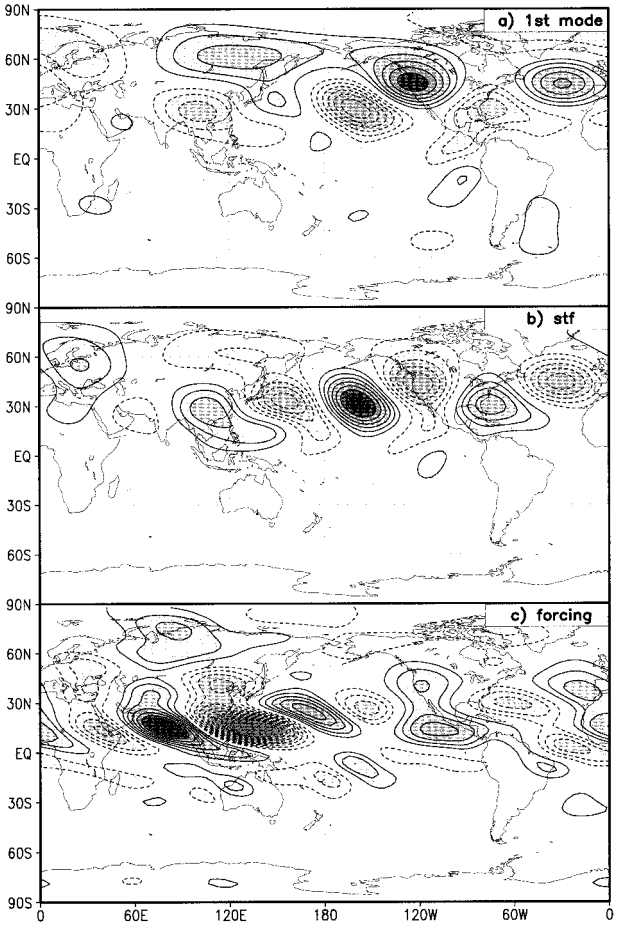

FIG. 10. (a) The dominant eigenmode of the linear model for the 1989 basic state. The dominant SVD of (b) the streamfunction and (c) the forcing for the 1989 basic state with white noise forcing. Contour intervals are arbitrary.

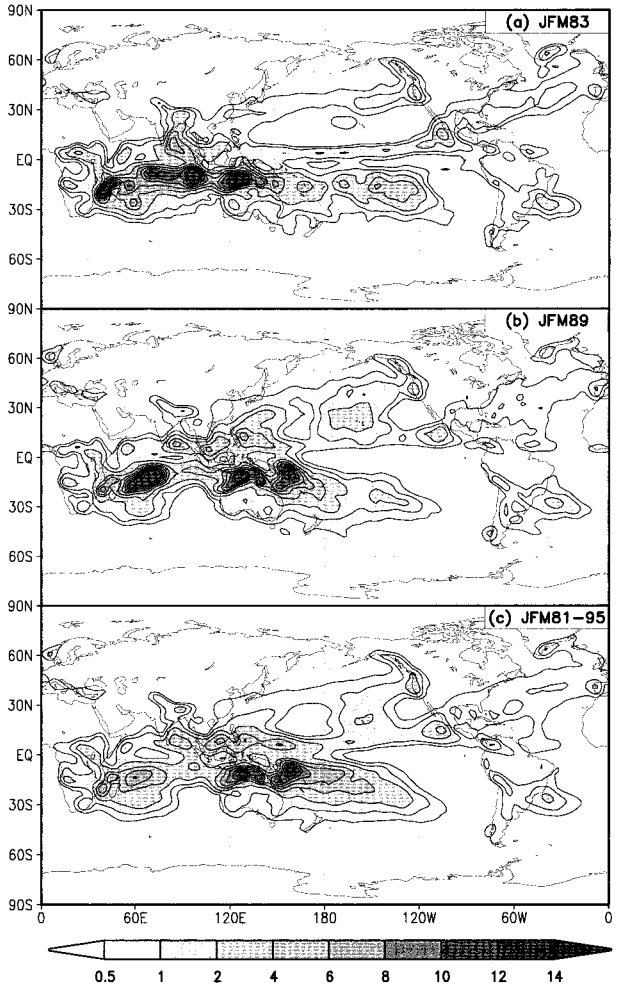

FIG. 11. The global distribution of the AGCM noise (intraensemble variance) of the JFM precipitation based on (a) the 27 ensemble members for 1983, (b) the 27 ensemble members for 1989, and (c) the 9-member ensembles covering the period 1981–95. Units: mm^2 day^{-2}.

functions by drawing random numbers and multiplying them by the standard deviation of precipitation times the Coriolis parameter. Poleward of 20°, where the relationship between precipitation anomalies and effective vorticity sources is not readily approximated, forcing is set to zero. As before, we generate noise that is white in space—albeit modulated by the envelope of tropical precipitation standard deviation—and repeat the calculation 500 times to generate the intra-ensemble variances of the solutions.

As a preliminary step to assessing the impact of the interannual changes in the variability of the tropical forcing, we repeat the calculations of the previous section, but instead of using the global homogeneous white noise forcing, we apply the control tropical precipitation envelope to the forcing (as described above) for all three basic states. Here, we are interested in seeing whether the strong sensitivity to the basic state found in the previous section is retained when the forcing is confined to the Tropics. Also, by using the envelope forcing, these solutions serve as an important reference for the following calculations in which we assess the impact of different envelope forcings. Figure 12 shows the results for each year's basic state relative to the control basic state. It is clear that the results are very similar to those with the global homogeneous forcing (cf. Fig. 9). The 1989 basic-state solutions have variability more than a factor of 2 larger than that of the control over a number of regions of the Pacific, North American, and the North Atlantic, coinciding with the dominant eigenmode (Fig. 10a). For 1983, variance is increased over the North and South Pacific, and much of the Atlantic.

We next assess the impact of the interannual changes in the variability of the tropical forcing. For each year's basic state, solutions are computed using the precipitation envelope for that year. These are compared in Fig. 13 against the solutions with each year's basic state but with the control precipitation envelope discussed previously (our reference solutions). For 1983, the impact

Unauthenticated | Downloaded 03/16/25 08:33 PM UTC

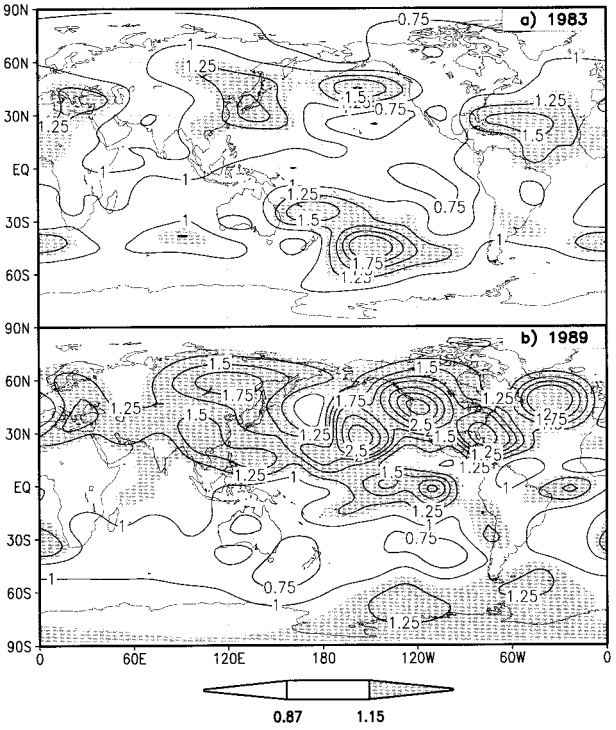

FIG. 12. Results from the linear models showing the impact of the different basic states. The forcing is confined to the region equatorward of 20° and has the control precipitation envelope applied. See text for details. (a) The ratio of the variance of the solutions with the 1983 basic state to the variance of the solutions with the control basic state. (b) The ratio of the variance of the solutions with the 1989 basic state to the variance of the solutions with the control basic state.

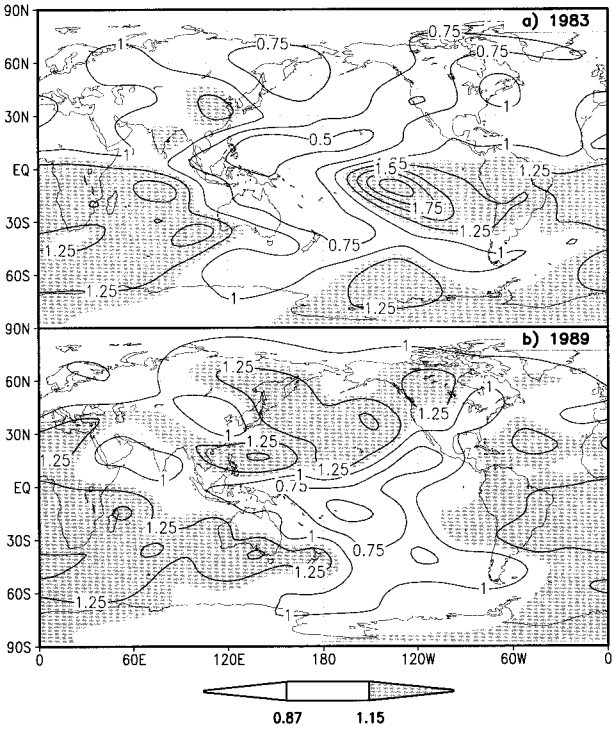

FIG. 13. Results from the linear models showing the impact of the AGCM precipitation envelopes. (a) The ratio of the variance of 1983 basic state with the 1983 precipitation envelope solutions to the variance of the 1983 basic state with the control (1981–95) precipitation envelope solutions. (b) The ratio of the variance of 1989 basic state with the 1989 precipitation envelope solutions to the variance of the 1989 basic state with the control (1981–95) precipitation envelope solutions.

of the change in precipitation variability is to reduce the response by more than 25% (as compared with the control precipitation envelope) over much of the PNA region. Reduced variability extends across much of the western tropical Pacific and South Pacific. A substantial increase in variability occurs primarily over the eastern tropical Pacific (a factor of 2 locally), with smaller increases over the rest of the Tropics, especially over the Indian Ocean. For 1989, the impact of the precipitation variability on the extratropics is largely opposite to that for 1983. An increase in variability of more 25% occurs over much of the PNA region. Reduced variability is largely confined to the central and eastern tropical Pacific (over the cold water of La Niña) and regions extending poleward and eastward across the eastern United States and the southern tip of South America.

To assess the sensitivity of the results shown in Fig. 13 to the basic state, we repeat the above experiments, but instead of using each year's basic state, we use the control basic state with each year's envelope forcing. In this case, our reference solutions are those with both the control envelope forcing and the control basic state. The results (not shown) are very similar, indicating that the sensitivity of the response to different forcings is independent of the basic state used, as long as we compare only cases using the same basic state.

c. Impact of submonthly transients

We next consider the impact of interannual differences in the AGCM's submonthly transients on the extratropical mean response. In this case, an envelope is applied to the baseline forcing based on the standard deviation of the submonthly vorticity flux divergence (not shown). Specifically, the random numbers are multiplied by the standard deviation of the vorticity flux divergence equatorward of 60°. Comparing the result (Fig. 14a) of forcing the 1983 basic-state model with forcing distributions based on control and 1983 vorticity flux divergence envelopes, we find the impact in the extratropics is typically less than 30%, with generally reduced variability over the PNA region. The impact is substantial for the 1983 basic state (Fig. 14a) only in the eastern tropical Pacific where the impact exceeds 50% (see also Fig. 12a). A similar calculation using the 1989 basic state and 1989 vorticity flux distribution indicates (Fig. 14b) the change in the variance of vorticity fluxes in that year too may have made a small contribution to the midlatitude low-frequency noise found in

Unauthenticated | Downloaded 03/16/25 08:33 PM UTC

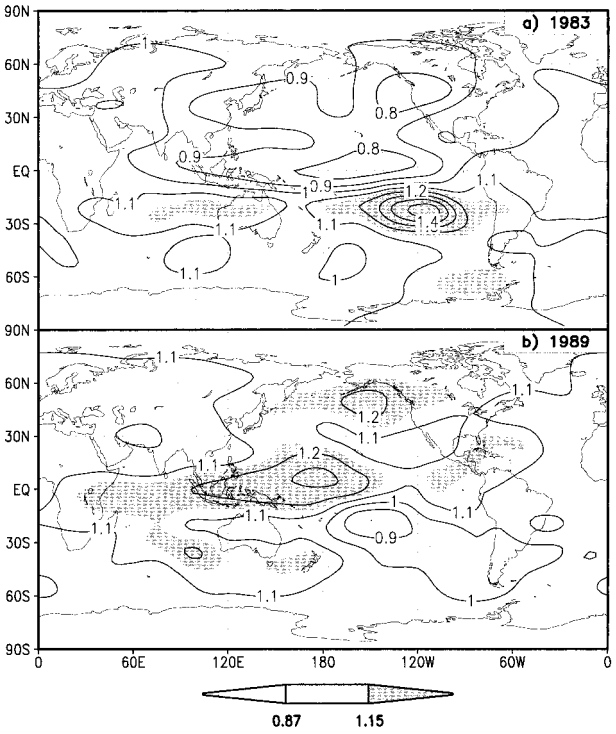

FIG. 14. Results from the linear models showing the impact of the AGCM submonthly vorticity flux divergence envelope applied equatorward of 60°. See text for details. (a) The ratio of the variance of 1983 basic state with the 1983 vorticity flux divergence envelope solutions to the variance of the 1983 basic state with the control (1981–95) vorticity flux divergence envelope solutions. (b) The ratio of the variance of 1989 basic state with the 1989 vorticity flux divergence envelope solutions to the variance of the 1989 basic state with the control (1981–95) vorticity flux divergence envelope solutions.

that year. We note that this does not rule out the possibility that differences in the structure of the transients could be important, though we do not consider that possibility here.

5. Summary and conclusions

In this study we examined how the variability in extratropical seasonal mean forecasts is affected by interannual differences in the background state, tropical forcing, and subseasonal transients associated with the 1983 El Niño and 1989 La Niña events. The analysis was based on two sets (one for each year) of 27 hindcasts generated from 15 December perturbed initial conditions, using the GEOS-2 atmospheric general circulation model (AGCM) and sea surface temperatures (SSTs) specified from observations. The forecast variability or noise was estimated from the intra-ensemble variability of the 27 January–February–March (JFM) mean hindcasts. A stochastically forced barotropic model linearized about the AGCM's 1983 and 1989 basic states was used to further assess the mechanisms modulating the uncertainties in the seasonal forecasts.

The AGCM results show that there are pronounced differences in the magnitude of the extratropical seasonal mean noise during these two years. The North Pacific, in particular, shows extensive regions where the 1989 JFM mean noise kinetic energy (SKE) is more than 2 times that of the 1983 forecasts. These differences in variability are highly significant and reflect the large contribution of the Pacific–North American (PNA) pattern to the noise of the 1989 JFM hindcasts. A diagnostic analysis of the SKE shows that the larger North Pacific values in 1989 are associated with a larger barotropic conversion of kinetic energy from the mean Pacific jet to the seasonal mean noise. During 1983, both the SKE and conversion over the North Atlantic are larger than in 1989. The increased PNA variability and generation of SKE by the mean flow during 1989 are consistent with the results of Chen and van den Dool (1997). That study showed that blocking and deep trough flows develop 2 times as often over the North Pacific during La Niña winters as compared with El Niño winters. They also found an important contribution to the low-frequency variability from high-frequency transients (in high latitudes): the current results suggest a minor role for these transients. It is unclear whether these differences represent model dificiencies or whether they are indicative of sampling variability.

As mentioned earlier, the current model has a rather weak JFM mean ENSO response, and we must question whether that leads to unrealistic noise estimates. Comparisons of the noise in the GEOS-2 AGCM with that of five other AGCMs (Shukla et al. 2000) suggests, however, that is not the case. In fact, the GEOS-2 noise estimates are comparable to those of several other models with considerably stronger ENSO responses over the PNA region. Nevertheless, the issue of model dependence is an important concern. Kumar et al. (2000) examined four different AGCMs and found a significant but small decrease in variability over the North Pacific for warm ENSO conditions and little change for cold conditions. That study, however, was based on a composite of all warm and cold events during 1950–94. We suggest that the smaller impact found in that study may be in part the result of compositing events with different seasonal mean extratropical responses (e.g., Palmer and Mansfield 1986), and therefore different mean flow kinetic energy conversions. Sardeshmukh et al. (2000), for example, found an increase in variability in the geopotential height response over the North Pacific for both the 1989 cold and 1987 warm event compared with neutral ENSO conditions. Clearly, further work is needed to sort out differences in variability resulting from model differences.

Our analysis of the timescales of the seasonal mean noise suggests that the noise is not generated at these very long (seasonal) timescales, but that it is for the most part statistically indistinguishable from variability that is uncorrelated from one month to the next. This interpretation of the seasonal mean variability as a sta-

Unauthenticated | Downloaded 03/16/25 08:33 PM UTC

tistical residue of shorter timescales is further supported by the similarity of the kinetic energy conversions computed from the seasonal and monthly data.

The importance of the differences in the basic states in the generation of SKE was confirmed with the linear model. When forced globally with homogeneous, spatially white noise, the linear model generates variance over the North Pacific for the 1989 basic state that is more than a factor of 2 larger than for the 1983 basic state. The 1989 variability is dominated by a single eigenmode, and it is strongly coupled with forcing over the tropical western Pacific and the Indian Ocean. We note that a number of previous studies have identified perturbations in the western Pacific and Indonesian regions as being particularly efficient at exciting an extratropical response (e.g., Simmons et al. 1983).

In addition to differences in the basic states, the SKE is also potentially impacted by interannual differences in the intraensemble noise in the tropical forcing and submonthly transients. The impact of the tropical forcing was examined in the linear model by modifying the variance of the global white noise forcing to include an envelope based on the AGCM JFM intraensemble precipitation variance equatorward of 20°. The results show a modest impact over the North Pacific and North America, with about a 25% reduction in variance for 1983 and a 25% increase in variance for 1989 as compared with the control. The impact of the subseasonal transients was determined by applying an envelope to the white noise forcing based on the variance of the AGCM submonthly vorticity flux divergence equatorward of 60°. These results also show only a modest impact over the North Pacific and North America, with about a 20% reduction in variance for 1983 and a 20% increase in variance for 1989 compared with the control. For both the precipitation and submonthly transients, the greatest impact on the variability is confined to the tropical central and eastern Pacific. We note that Newman et al. (1997) suggest that it is important to include the space–time structure of the forcing to obtain improved barotropic model predictions of the wintertime flow, though that is not considered here.

We conclude that the increased variability in the GEOS-2 AGCM seasonal mean forecasts during 1989 compared with 1983 is largely due to the differences in the basic state. While these results are generally consistent with observations (Chen and van den Dool 1997), they must be tempered by the fact that there is considerable model dependence in the noise and signal in seasonal forecasts (e.g., Shukla et al. 2000). Our results further suggest that, in view of the large differences in the extratropical mean response to ENSO events, the analysis of composite events can give a misleading picture of the uncertainties associated with ENSO forecasts. Progress in this area will require more diagnostic studies of individual ENSO events based on ensembles of seasonal forecasts sufficiently large to obtain reliable estimates of second-order statistics.

Acknowledgments. We wish to thank Dr. Tom Bell for advice on the statistical significance tests. We also wish to thank the editor (Francis Zwiers), and two anomymous reviewers for their careful and insightful reviews. This work was carried out under the NASA Seasonal-to-Interannual Prediction Project with support from the NASA Earth Science Enterprises's Global Modeling and Analysis Program.

APPENDIX

Field Significance Tests

We establish the significance of the ratio of the 1989 to 1983 SKE (Fig. 3c) using a Monte Carlo technique. In this approach, synthetic data are produced with the same spatial covariance structure as that of the model output. This is important for establishing field significance (Livezey and Chen 1983). In particular, for each year synthetic wind data are constructed from the AGCM EOFs of the combined seasonal mean u and v wind anomalies as

$$x_i = \sum_i a_i \lambda_i E_i, \tag{A1}$$

where the E_i are the combined u and v EOFs of the AGCM's seasonal mean wind anomalies, the λ_i are the corresponding eigenvalues, and the a_i are independent realizations from a zero mean, unit normal distribution. We produce 10 000 realizations of 27 synthetic seasonal mean kinetic energy fields for each year (normalized by the AGCM KE of the appropriate year). These realizations provide estimates of the sampling distribution of the variance ratio under the null hypothesis (variances are the same for 1983 and 1989), and are used to determine the critical 5% local significance values, as well as the field significance of the 5% area. The results show that the points where the SKE ratio is greater (less) than 1.6 (.64) are locally significant at the 5% level (one sided). We note that this is consistent with the traditional F test based on 52 degrees of freedom. This indicates that we can consider u and v as being approximately independent for this test (26 degrees of freedom from each wind component). We find from the AGCM output that, 28.2% of the area in Fig. 3c has values of the ratio greater than 1.6, while only 8.7% of the area has values less than 0.64. The field significance test shows that the 28.2% value is significant (values greater than 20% are significant at the 5% level), while the 8.7% value is not significant (only values greater than 22% are significant at the 5% level).

The field significance of the ratios in Fig. 6 is determined as follows. The basic test statistic is the ratio of the variance of the seasonal means to one-third the variance of the monthly means. The seasonal cycle is removed from the variance estimates of the monthly means by computing the variances separately for each calender month (January, February, and March): these are then averaged together. We test whether the ratio of

Unauthenticated | Downloaded 03/16/25 08:33 PM UTC

the variance of the seasonal means to one-third the variance of the monthly means is significantly different from one by using the same basic Monte Carlo approach outlined above. In this case, the synthetic wind data are produced from the EOFs of the combined *monthly* mean wind anomalies. For each year, we generate 3000 realizations of 27×3 synthetic monthly mean wind fields. For each realization, 27 synthetic seasonal means are computed by averaging 3-monthly mean fields. These synthetic monthly and seasonal mean wind fields are then used to construct 3000 samples of the ratio of the kinetic energy of the seasonal means to one-third the kinetic energy of the monthly means. The results of the 3000 Monte Carlo simulations indicate that the grid points where the ratio is greater (less) than 1.27 (0.75) are locally significant at the one-sided 5% level. Furthermore, for both years, areas with local significance must be greater than one-fifth of the total area to have field significance.[1] For 1983 (Fig. 6c), we find that 26% (2.2%) of the area has values that are larger than 1.27 (smaller than 0.75). For 1989 (Fig. 6d), we find that 25% (5.7%) of the area has values that are larger than 1.27 (smaller than 0.75). Thus, in both years the areas with values exceeding 1.27 are field significant at the 5% level.

REFERENCES

Arkin, P., 1989: The global climate for December 1988–February 1989: Cold episode in the tropical Pacific continues. *J. Climate,* **2,** 737–757.

Barnett, T. P., 1995: Monte Carlo climate forecasting. *J. Climate,* **8,** 1005–1022.

Borges, M. D., and P. D. Sardeshmuhk, 1995: Barotropic Rossby wave dynamics of zonally varying upper-level flows during northern winter. *J. Atmos. Sci.,* **52,** 3779–3796.

Branstator, G., 1985: Analysis of general circulation model sea-surface temperature anomaly simulations using a linear model. Part I: Forced solution. *J. Atmos. Sci.,* **42,** 2225–2241.

——, 1990: Low-frequency patterns induced by stationary waves. *J. Atmos. Sci.,* **47,** 629–648.

——, 1995: Organization of storm track anomalies by recurring low-frequency circulation anomalies. *J. Atmos. Sci.,* **52,** 207–226.

Bretherton, C. S., C. Smith, and J. M. Wallace, 1992: An intercomparison of methods for finding coupled patterns in climate data. *J. Climate,* **5,** 541–560.

Chang, Y., S. D. Schubert, and M. J. Suarez, 2000: Boreal winter predictions with the GEOS-2 GCM: The role of boundary forcing and initial conditions. *Quart. J. Roy. Meteor. Soc.,* **126,** 2293–2321.

Chen, W. Y., and H. M. van den Dool, 1997: Asymmetric impact of tropical SST anomalies on atmospheric internal variability over the North Pacific. *J. Atmos. Sci.,* **54,** 725–740.

DeGroot, M. H., 1975: *Probability and Statistics*. Addison-Wesley, 607 pp.

Dymniikov, V. P., and A. N. Filatov, 1989: On problem of stability of quasi-stationary equivalent barotropic atmospheric flows. *Sov. J. Numer. Anal. Math. Mod.,* **4,** 227–238.

Feldstein, S. B., 2000: The timescale, power spectra, and climate noise properties of teleconnection patterns. *J. Climate,* **13,** 4430–4440.

Held, I. M., S. W. Lyons, and S. Nigam, 1989: Transients and the extratropical response to El Niño. *J. Atmos. Sci.,* **46,** 163–174.

Hoskins, B. J., I. N. James, and G. H. White, 1983: The shape propagation and mean flow interaction of large-scale weather systems. *J. Atmos. Sci.,* **40,** 1595–1612.

Klinker, E., and P. D. Sardeshmukh, 1992: The diagnosis of mechanical dissipation in the atmosphere from large-scale balance requirements. *J. Atmos. Sci.,* **49,** 608–627.

Kok, C. J., and J. D. Opsteegh, 1985: Possible causes of anomalies in seasonal mean circulation patterns during the 1982–83 El Niño event. *J. Atmos. Sci.,* **42,** 677–694.

Kumar, A., and M. P. Hoerling, 1995: Prospects and limitations of seasonal atmospheric GCM predictions. *Bull. Amer. Meteor. Soc.,* **76,** 335–345.

——, A. Barnston, P. Peng, M. Hoerling, and L. Goddard, 2000: Changes in the spread of the variability of the seasonal mean atmospheric states associated with ENSO. *J. Climate,* **13,** 3139–3151.

Livezey, R. E., and W. Y. Chen, 1983: Statistical field significance and its determination by Monte Carlo techniques. *Mon. Wea. Rev.,* **111,** 46–59.

Newman, M., P. D. Sardeshmukh, and C. Penland, 1997: Stochastic forcing of the wintertime extratropical flow. *J. Atmos. Sci.,* **54,** 435–455.

Palmer, T. N., 1988: Medium and extended range predictability, stability of the PNA mode, and atmospheric response to sea surface temperature anomalies. *Quart. J. Roy. Meteor. Soc.,* **114,** 691–713.

——, and D. A. Mansfield, 1986: A study of wintertime circulation anomalies during past El Niño events using a high resolution general circulation model. II: Variability of the seasonal mean response. *Quart. J. Roy. Meteor. Soc.,* **112,** 639–660.

Quiroz, R. S., 1983: The climate of the ''El Niño'' winter of 1982–83—A season of extraordinary climate anomalies. *Mon. Wea. Rev.,* **111,** 1685–1706.

Reynolds, W. R., and D. S. Marsico, 1993: An improved real-time global sea surface temperature analyses. *J. Climate,* **6,** 114–119.

Sardeshmukh, P. D., M. Newman, and M. D. Borges, 1997: Free barotropic Rossby wave dynamics of the wintertime low-frequency flow. *J. Atmos. Sci.,* **54,** 5–23.

——, G. P. Combo, and C. Penland, 2000: Changes of probability associated with El Niño. Preprints, *Eighth Conf. on Climate Variations,* Denver, CO, Amer. Meteor. Soc., 16–19.

Schubert, S. D., 1986: The structure, energetics and evolution of the dominant frequency-dependent three-dimensional atmospheric modes. *J. Atmos. Sci.,* **43,** 1210–1237.

——, and M. J. Suarez, 1989: Dynamical predictability in a simple general circulation model: Average error growth. *J. Atmos. Sci.,* **46,** 353–370.

——, R. B. Rood, and J. Pfaendtner, 1993: An assimilated data set for earth science applications. *Bull. Amer. Meteor. Soc.,* **74,** 2331–2342.

Shukla, J., and Coauthors, 2000: Dynamical seasonal prediction. *Bull. Amer. Meteor. Soc.,* **81,** 2593–2606.

Simmons, A. J., J. M. Wallace, and G. Branstator, 1983: Barotropic wave propagation and instability, and atmospheric teleconnection patterns. *J. Atmos. Sci.,* **40,** 1363–1392.

Wallace, J. M., and D. S. Gutzler, 1981: Teleconnections in the geopotential height field during the Northern Hemisphere winter. *Mon. Wea. Rev.,* **109,** 784–812.

[1] The one-sided percentages obtained from the Monte Carlo simulations ranged betwen 19% and 21% for 1983 and 1989 and for the upper and lower 5% levels.

Unauthenticated | Downloaded 03/16/25 08:33 PM UTC